

Minimax Active Learning

Sayna Ebrahimi, William Gan, Kamyar Salahi, Trevor Darrell
UC Berkeley

{sayna, wjgan, kam.salahi, trevordarrell}@berkeley.edu

Abstract

Active learning aims to develop label-efficient algorithms by querying the most representative samples to be labeled by a human annotator. Current active learning techniques either rely on model uncertainty to select the most uncertain samples or use clustering or reconstruction to choose the most diverse set of unlabeled examples. While uncertainty-based strategies are susceptible to outliers, solely relying on sample diversity does not capture the information available on the main task. In this work, we develop a semi-supervised minimax entropy-based active learning algorithm that leverages both uncertainty and diversity in an adversarial manner. Our model consists of an entropy minimizing feature encoding network followed by an entropy maximizing classification layer. This minimax formulation reduces the distribution gap between the labeled/unlabeled data, while a discriminator is simultaneously trained to distinguish the labeled/unlabeled data. The highest entropy samples from the classifier that the discriminator predicts as unlabeled are selected for labeling. We extensively evaluate our method on various image classification and semantic segmentation benchmark datasets and show superior performance over the state-of-the-art methods.¹

1. Introduction

The outstanding performance of modern computer vision systems on a variety of challenging problems [14] is empowered by several factors: recent advances in deep neural networks [11], increased computing power [10], and an abundant stream of data [33], which is often expensive to obtain. Active learning focuses on reducing the amount of human-annotated data needed to obtain a given performance by iteratively selecting the most *informative* samples for annotation.

Notably, a large research effort in active learning, implicitly or explicitly, leverages the uncertainty associated with

¹Project page: <https://people.eecs.berkeley.edu/~sayna/mal.html>

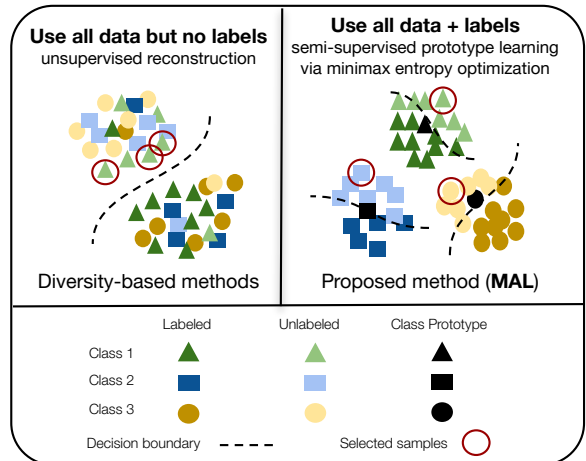


Figure 1: **Left:** Diversity-based task-agnostic active learning approaches perform unsupervised learning on all data and adversarially train a discriminator to predict whether to label a sample. The red-circled samples show a failure case for such methods, where the unlabeled samples closest to the discriminator’s decision boundary are all from the same class and do not provide a diverse set of data to label. **Right:** Our proposed approach (MAL) performs semi-supervised learning on all data and uses the label information to learn per-class prototypes and then train a binary classifier to predict which samples to label. In contrast to the diversity-based approach, the selected red-circled samples are chosen because they are farther from the class prototypes, and as a result, come from different classes.

the outcomes on the main task for which we are trying to annotate the data [66, 32, 18, 23, 68, 4]. These approaches are vulnerable to outliers and are prone to annotate redundant samples in the beginning because the task model is equally uncertain on almost all the unlabeled data, regardless of how representative the data are for each class [56]. As an alternative direction, [56] introduced a *task-agnostic* approach in which they applied reconstruction as an unsupervised task on the labeled and unlabeled data, which allowed for train-

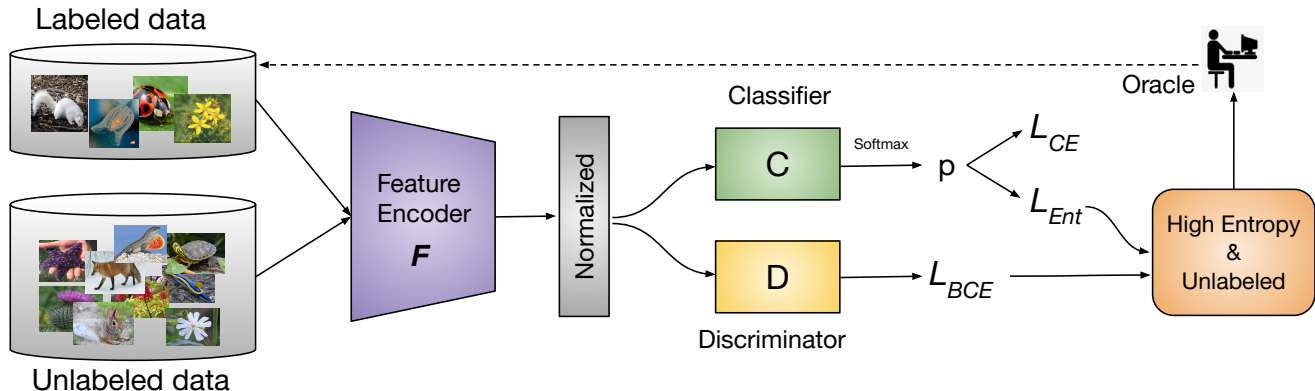


Figure 2: The MAL pipeline: both labeled and unlabeled data are input into a common feature encoder F , followed by a normalization layer and a cosine similarity-based classifier C which is trained to maximize entropy on unlabeled data, whereas F is trained to minimize it. We also train a discriminator D (a binary classifier) to predict *labeledness* of the data. Samples with highest entropy from the classifier that the discriminator predicts as unlabeled are selected for labeling.

ing a discriminator adversarially to predict whether a given sample should be labeled.

Task-agnostic approaches achieve strong performance on a variety of datasets [56] and can select new samples for labeling without requiring updated annotations from the labeler, i.e. because task-agnostic approaches do not use the annotations. But by ignoring the annotations, task-agnostic approaches disregard how similar the unlabeled samples are to the labeled sample classes. As a result, the samples selected by the task-agnostic discriminator can all come from the same class, even if there is already a high proportion of labeled samples from that class. Figure 1 (left) shows this failure case for task-agnostic approaches, while Figure 1 (right) shows how taking into account annotation information can alleviate this problem.

In this paper, we empirically show that the performance increase from using all data as well as all labels can be crucial in real-world settings where datasets are imbalanced and poor performance on a specific class can be highly correlated with having fewer labeled samples for that class. Therefore, ranking the unlabeled data with respect to its entropy in addition to its *labeledness* score can guide the acquisition function to not only query samples that *do not look similar to what has been seen before*, but also rank them based on *how far they are from the predicted class prototypes*.

This paper introduces a semi-supervised pool-based task-aware active learning algorithm that combines the best of both directions in active learning literature. Our approach, called Minimax Active Learning (MAL), queries samples based on their *diversity* as well as their *uncertainty* scores obtained by a distance-based classifier trained on the main task. The diversity or *labeledness* of the data is pre-

dicted by a discriminator that is trained to distinguish between the labeled and unlabeled features generated by an encoder that optimizes a minimax objective to reduce intra-class variations in the dataset. Given two sets of labeled and unlabeled data, it is difficult to train a classifier that can distinguish between them without overfitting to the dominant set (unlabeled pool). Our key idea is to learn a latent space representation which is adversarially trained to become discriminative while we minimize the expected loss on the labeled data.

Figure 2 illustrates our model architecture. In particular, MAL has three major building blocks: (i) a feature encoder (F) that attempts to minimize the entropy of the unlabeled data for better clustering. (ii) a distance-based classifier (C) that adversarially learns per-class weight vectors as prototypes and attempts to maximize the entropy of the unlabeled data (iii) a discriminator that uses features generated by F to predict which pool each sample belongs to. Inspired by recent advances in few-shot learning, we use a distance-based classifier to learn per-class weighted vectors as prototypes (similar to prototypical [57] and matching networks [65]) using cosine similarity scores [8]. To leverage the unlabeled data, we perform semi-supervised learning using entropy as our optimization objective which is easy to train and does not require labels.

While the feature extractor minimizes the entropy by pushing the unlabeled samples to be clustered near the prototypes, the classifier increases the entropy of the unlabeled samples, and hence makes them similar to all class prototypes. On the other hand, they both learn to classify the labeled data using a cross-entropy loss, enhancing the feature space with more discriminative features. We train a binary discriminator on this space to predict *labeledness* for each

example and at the end samples which (i) are predicted as unlabeled with high confidence by the discriminator and (ii) achieved high entropy by the classifier C will be sent to the oracle.

While distance-based classification [45, 48, 8] and min-max entropy for image classification [28, 37, 25, 50, 59] have been studied before, to the best of our knowledge, our work is the first to use them together for active learning. This work is also the first to show semi-supervised learning with minimax entropy for semantic segmentation. Our results demonstrate significant performance improvements on a variety of image classification benchmarks such as CIFAR100, ImageNet, and iNaturalist2018 and on semantic segmentation using the BDD100K driving dataset.

2. Related Work

Active learning: Recent work in active learning can be divided into two sets of approaches: query-synthesizing (generative) methods or query-acquiring (pool-based) methods. Query-synthesizing methods produce informative synthetic samples using generative models [41, 43, 73, 61] while pool-based approaches focus on selecting the most informative samples from a data pool. We focus chiefly on the latter line of research.

Pool-based methods have been shown both theoretically and empirically to achieve better performance than Random sampling [53, 16, 20]. Among pool-based methods, there exist three major categories: uncertainty-based approaches [23, 68, 4], representation-based (or diversity) approaches [51, 66, 56], and hybrid approaches [70, 47, 2]. Pool-based sampling strategies have been studied widely with early works such as information-theoretic methods [40], ensembles methods [44, 16] and uncertainty heuristics [60, 39] surveyed by Settles [52].

Uncertainty-based pool-based methods have been studied in both Bayesian [18, 32] and non-Bayesian settings. Some Bayesian approaches have leveraged Gaussian processes or Bayesian neural networks [29, 49, 12] for uncertainty estimation. Gal et al. [18, 17] demonstrated that Monte Carlo (MC) dropout can be used for approximate Bayesian inference for active learning on small datasets. However, as discussed in later works [51, 32], Bayesian techniques often do not scale well to large datasets due to batch sampling. In the non-Bayesian setting, uncertainty heuristics such as distance from the decision boundary, highest entropy, and expected risk minimization have been widely investigated [6, 60, 69]. Ensembles have shown to be successful in representing uncertainty [38, 70] and can outperform MC dropout approaches [5].

Diversity-based methods focus on sampling images that represent the diversity in a set of unlabeled images. Sener et al. [51] proposed a core-set approach for sampling diverse points by solving the k-Center problem in the last-

layer embedding of a model. They also produced a theoretical bound on core-set loss that scales with the number of classes, meaning that performance deteriorates as class size increases. Furthermore, with high-dimensional data, distance-based representations including core-set often suffer from a convergence of pairwise distances in high dimensions, known as the *distance concentration phenomenon* [15]. Variational adversarial active learning (VAAL) was proposed by [56] as a task-agnostic diversity-based algorithm that samples data points using a discriminator trained adversarially to discern labeled and unlabeled points on the latent space of a variational auto-encoder.

Hybrid approaches leverage both uncertainty and diversity. BatchBALD [32] was proposed as a tractable remedy for non-jointly informative sampling in BALD. Using a Monte Carlo estimator, BatchBALD approximates the mutual information between a batch of points and the model’s parameters and greedily generates a batch of samples. Rather than using model outputs as is standard for most uncertainty-based approaches, BADGE [2] utilizes the *gradient* of the predicted category with respect to the last layer of the model. These gradients provide an uncertainty measure as well as an embedding that can be clustered via k-means++ [1] initialization to select diverse points.

Although active learning research in semantic segmentation has been a bit more sparse, approaches largely parallel those of classification methods such as in the use of MC Dropout [23], feature entropy and conditional geometric entropy for uncertainty measures [34]. Diversity-based samplers like VAAL [56] were also shown to be effective on semantic segmentation. Recently, [7] proposed a deep reinforcement learning approach for selecting regions of images to maximize Intersection over Union (IoU).

Entropy regularization Entropy regularization has been widely used in parametric models of posterior probabilities to benefit from unlabeled data or partially labeled data [24]. Entropy was also proposed to be used for clustering data and training a classifier simultaneously [35]. In the field of domain adaptation, [62] used cross-entropy between target activation and soft labels to exploit semantic relationships in label space whereas [58] trained a discriminative classifier using unlabeled data by maximizing the mutual information between inputs and target categories. In [50], they used entropy optimization for semi-supervised domain adaptation. Recently [67] proposed a fully test-time adaptation method that performs entropy minimization to adapt to the test data at inference time.

Adversarial learning Adversarial learning has been used for different problems such as generative modeling models [22], object composition [3], representation learning [42], domain adaptation [63], continual learning [13], and active learning [56]. The use of an adversarial network enables the model to train in a fully-differentiable man-

ner by adjusting to solve the *minimax* optimization problem [22]. In this work, we perform the minimax between a feature encoder and a classifier using Shannon entropy [54].

3. Minimax Active Learning

In this section, we introduce MAL formulation for image classification and semantic segmentation settings. Our training procedure is shown in Algorithm 1.

We consider the problem of learning a label-efficient model by iteratively selecting the most *informative* samples from a given *split* to be labeled by an oracle or a human expert. We start with an initial small pool of labeled data denoted as $\mathcal{L} = \{(x_L^i, y_L^i)\}_{i=1}^{N_L}$, and a large pool of unlabeled data denoted as $\mathcal{U} = \{x_U^i\}_{i=1}^{N_U}$ where our goal is to populate a fixed sampling *budget*, b , using an acquisition strategy to query samples from the unlabeled pool ($x_U \sim X_U$) such that the expected loss is minimized.

3.1. MAL for image classification

MAL starts with encoding data using a convolutional neural network (CNN), denoted as F , to a d -dimensional latent vector where features are normalized using an ℓ_2 normalization. Similar to [8] in few-shot learning and [50] in domain adaption, we exploit a cosine similarity-based classifier denoted as C and parametrized by the weight matrix $\mathbf{W} \in \mathbb{R}^{d \times K}$, which takes the normalized features as input and maps them to K class prototype vectors $[\mathbf{w}_1, \mathbf{w}_2, \dots, \mathbf{w}_K]$, where K is the total number of classes in the dataset. The outputs of C are converted to probability values $\mathbf{p} \in \mathbb{R}^K$ using a Softmax function (σ). We first train F and C by performing a K -way classification task on the already labeled data using a standard cross-entropy loss shown below

$$\mathcal{L}_{CE} = -\mathbb{E}_{(x_L, y_L) \sim \mathcal{L}} \sum_{k=1}^K \mathbb{1}_{[k=y_L]} \log\left(\sigma\left(\frac{1}{T} \frac{\mathbf{W}^T F(x_L)}{\|F(x_L)\|}\right)\right) \quad (1)$$

where the subscript $i = \{1, \dots, N\}$ is dropped for simplicity. Eq. 1 learns the weight vectors \mathbf{w} for each class by computing entropy which represents cosine similarity between each \mathbf{w} and the output of the feature extractor.

Our key idea is to learn a discriminative feature space by minimizing the intraclass distribution gap on the unlabeled data by adversarially maximizing the entropy so that all samples have equal distance to all prototypes. We formulate this minimax game using Shannon entropy [54]:

$$\mathcal{L}_{Ent} = \min_F \max_C \left(- \sum_{k=1}^K p(y = k|x_U) \log p(y = c|x_U) \right) \quad (2)$$

where we first minimize the entropy in F , and that is minimizing the cosine similarity score between unlabeled samples associated with the same prototype, which results in a

more discriminative representation. Next, we maximize entropy in C , hence making a more uniform feature space. To achieve the adversarial learning, the sign of gradients for entropy loss on unlabeled samples is flipped by a gradient reversal layer [19].

The end goal of this minimax game is to generate a mixture of latent features associated with the labeled and unlabeled data, where a discriminator can be trained to map the latent representation to a binary label, which is 1 if the sample belongs to \mathcal{L} and is 0 otherwise. We call this binary classifier D and use a standard binary cross-entropy loss to train it.

$$\mathcal{L}_{BCE} = -\mathbb{E}\left[\log\left(\frac{1}{T} \frac{F(x_L)}{\|F(x_L)\|}\right)\right] - \mathbb{E}\left[\log\left(1 - \frac{1}{T} \frac{F(x_U)}{\|F(x_U)\|}\right)\right] \quad (3)$$

As shown in Algorithm 3, at the end of each split, we train a model with the collected data and report our performance. We first initialize the *task model*, denoted as M , using a pre-trained feature extractor F from the MAL training process and use it to continually learn all the collected splits.

3.2. MAL for semantic segmentation

For semantic segmentation, MAL similarly starts with encoding data using a convolutional neural network (F). However, the output is now a $d \times h \times w$ latent tensor where h and w are the height and width of the output filters, respectively as the segmentation task requires spatial information. After ℓ_2 normalization, we pass this tensor through a classifier C , which uses K prototype convolution filters $[\mathbf{w}_1, \mathbf{w}_2, \dots, \mathbf{w}_K]$ to produce a $K \times h \times w$ tensor. This tensor is then upsampled to the original image size and converted to probability tensor using the Softmax function, the result being $K \times H \times W$ where H and W are the height and width of the input images, respectively. F and C are trained using a pixel-average cross-entropy loss, where here the label is a $H \times W$ segmentation map.

To learn a discriminative feature space, we similarly train F to minimize entropy and adversarially train C to maximize it. However, in this formulation, entropy is taken to be the pixel-average in the output. To have our latent feature space contain *labeledness* information, we again train a discriminator as in above, but our discriminator model now takes in $d \times h \times w$ tensors as input and outputs a binary prediction for whether or not a sample is labeled.

3.3. Sampling strategy in MAL

The sampling strategy in MAL is shown in Algorithm 2. The key idea to our approach is that we have two conditions to select a sample for labeling. (1) We use the probability associated with the discriminator’s predictions as a score to rank samples based on their *diversity*, which can be interpreted as how similar they are to previously seen data. The

Algorithm 1 Minimax Active Learning (MAL)

Input: Labeled pool \mathcal{L} , Unlabeled pool \mathcal{U} , Initialized models for $\theta_F, \theta_C, \theta_D$

Input: Hyperparameters: epochs, $M, \alpha_1, \alpha_2, \alpha_3$

- 1: **for** $e = 1$ to epochs **do**
 - 2: sample $(x_L, y_L) \sim \mathcal{L}$
 - 3: sample $x_U \sim \mathcal{U}$
 - 4: Compute \mathcal{L}_{CE} by using Eq. 1
 - 5: $\theta'_F \leftarrow \theta_F - \alpha_1 \nabla \mathcal{L}_{CE}$
 - 6: $\theta'_C \leftarrow \theta_C - \alpha_2 \nabla \mathcal{L}_{CE}$
 - 7: Compute \mathcal{L}_{Ent} by using Eq. 2
 - 8: $\theta'_F \leftarrow \theta_F + \alpha_1 \nabla \mathcal{L}_{Ent}$
 - 9: $\theta'_C \leftarrow \theta_C - \alpha_2 \nabla \mathcal{L}_{Ent}$
 - 10: Compute \mathcal{L}_D by using Eq. 3
 - 11: $\theta'_D \leftarrow \theta_D - \alpha_3 \nabla \mathcal{L}_D$
 - 12: **end for**
 - 13: **return** Trained $\theta_F, \theta_C, \theta_D$
-

Algorithm 2 Sampling Strategy in MAL

Input: b, X_L, X_U

Output: X_L, X_U

- 1: Select samples (X_s) with $\min_b \{\theta_D(F(x))\}$ and $\max_b \{\theta_C(F(x))\}$
 - 2: $Y_o \leftarrow \text{ORACLE}(X_s)$
 - 3: $(X_L, Y_L) \leftarrow (X_L, Y_L) \cup (X_s, Y_o)$
 - 4: $X_U \leftarrow X_U - X_s$
 - 5: **return** X_L, X_U
-

closer the probability is to zero, the more confident D is that it comes from the unlabeled pool. (2) We use the entropy obtained by C on the unlabeled data and use it as a score to rank samples based on how far they are from class prototypes. We take the top b samples that meet both conditions. Unlike the uncertainty-based methods, our approach is not vulnerable to outliers as condition (1) prevents it because outliers never achieve a high confidence score from the discriminator because they are not similar to any samples that D has seen. On the other hand, unlike diversity-based approaches, MAL is task-aware and can identify unlabeled samples far from the learned class prototypes.

4. Experiments

In this section, we review the benchmark datasets and baselines used in our evaluation as well as the implementation details.

Datasets. We have evaluated MAL on two common vision tasks: image classification and semantic segmentation. For large-scale image classification, we have used **ImageNet** [9] with more than 1.2M images of 1000 classes and **iNaturalist2018** [64], which is a heavily imbalanced

Algorithm 3 Training for Main Task in MAL

Input: Labeled pool \mathcal{L} , Pre-trained F_θ from Alg. 1, M_θ

Input: Hyperparameters: epochs, α_4

- 1: Initialize M_θ with pre-trained F backbone
 - 2: **for** $e = 1$ to epochs **do**
 - 3: Compute \mathcal{L}_{CE} by using Eq. 1
 - 4: $\theta'_M \leftarrow \theta_M - \alpha_4 \nabla \mathcal{L}_{CE}$
 - 5: **end for**
 - 6: **return** M_θ
-

dataset with more than 430K natural images containing 8142 species. We have also used **CIFAR100** [36] with 60K images of size 32×32 as a popular benchmark in the field. To highlight the benefits of evaluating active learning algorithms in more realistic scenarios, we also created an imbalanced version of CIFAR100 (see Section 4.1). For semantic segmentation, we evaluate our method on **BDD100K** [72] which is a diverse driving video dataset with 8K images (7K for training and 1K for testing) and 19 classes with full-frame instance segmentation annotations collected from distinct locations in the United States. The statistics of these datasets are summarized in the appendix.

Baselines: we compare the performance of MAL against several other diversity and uncertainty based active learning approaches including VAAL [56], Coreset [51], Entropy [66], BALD [18]. We also show results for *Random sampling* in which samples are uniformly sampled at random, without replacement, from the unlabeled data and serves as a competitive baseline in active learning. To make an appropriate and fair comparison, we used the originally published code for all the baselines and integrated them into our code-base to ensure using identical data pools and training protocols.

Performance measurement. We evaluate the performance of MAL on the main task at the end of labeling predefined splits of the dataset using the task model M . In classification we use ResNet18 [27] for our M network and measure accuracy whereas, in segmentation, we compute mean IoU on the collected data where M is a dilated residual network (DRN) [71]. Algorithm 3 shows how we train M by initializing it with the feature extractor module (F) learned during MAL’s training which results in MAL achieving a higher mean accuracy *only by using the initial labeled pool and the unlabeled data before annotating any new instances*, compared to all the baselines in all the experiments (see Section 4.1 and 4.2. Results for all our experiments, except for ImageNet and CIFAR100-Imbalanced, are averaged over 5 runs. ImageNet and CIFAR100-Imbalanced results however, are obtained by averaging over 3 and 10 repetitions, respectively.

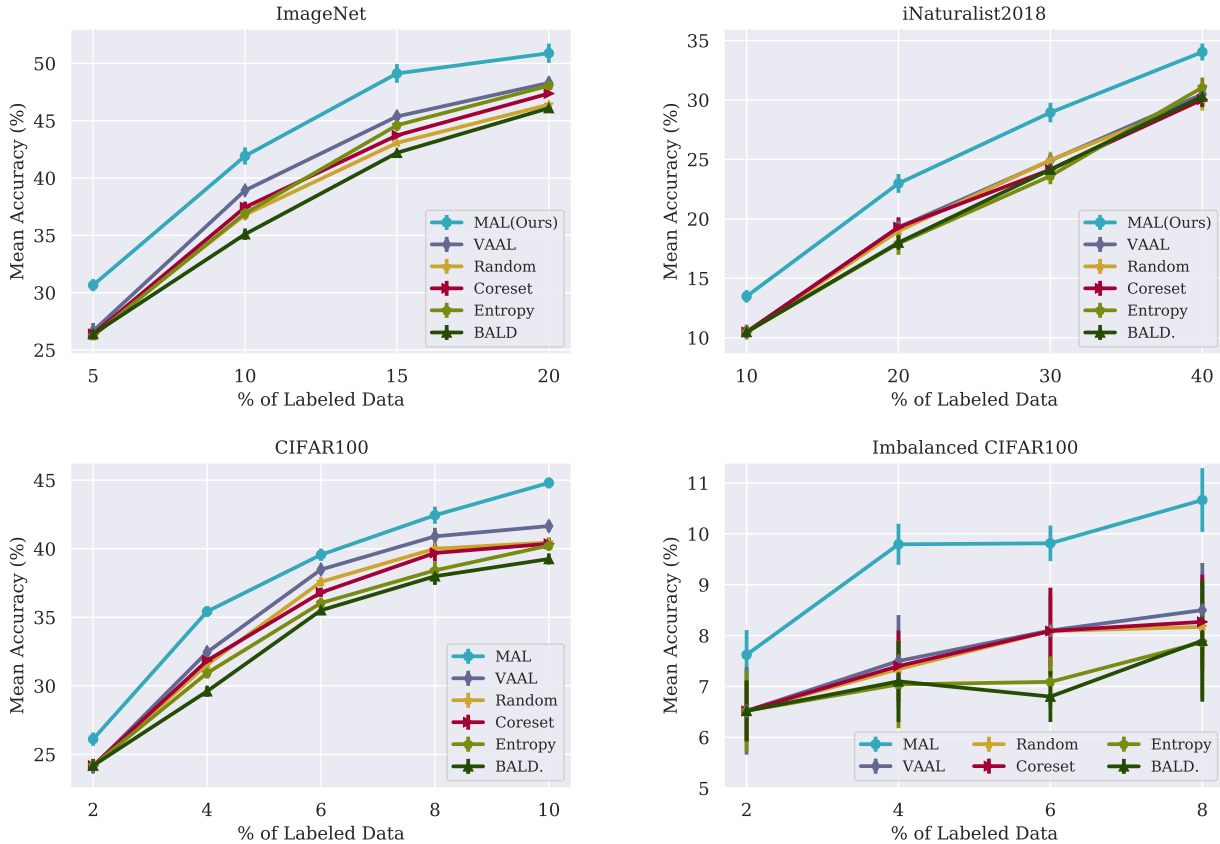


Figure 3: MAL performance on classification tasks using ImageNet and iNaturalist2018 (top row) and CIFAR100 and CIFAR100-Imbalanced (bottom row) compared to VAAL [56], Coreset [51], Entropy [66], BALD [18], and Random sampling. Best visible in color.

4.1. MAL on image classification benchmarks

Implementation details. Images in ImageNet and iNaturalist2018 are resized to 256 and then random-cropped to 224. We used random horizontal flips for data augmentation for all the datasets. For ImageNet, we used 5% of the entire dataset for the initial labeled pool and considered a budget size of 5% for each split. These numbers are both 10% for iNaturalist2018 and 2% for CIFAR100 dataset. The pool of unlabeled data contains the rest of the training set from which samples are selected to be annotated by the oracle. Once labeled, they will be added to the initial training set and training is repeated on the new training set. We assume the oracle is *ideal* and provides accurate labels. The architecture used in the task module for image classification is ResNet18 [27] with Xavier initialization [21]. The discriminator is a 3-layer multilayer perceptron (MLP) with ReLU non-linearities [46] and Adam [31] is used as the optimizer for F , C , and D . Training MAL continues for 60 epochs in ImageNet and iNaturalist2018 and for 100 epochs in CIFAR100.

MAL performance on ImageNet. Figure 3 shows mean accuracy obtained by our method (error are shown in error bars) compared to prior works and Random sampling for 4 splits from 5% – 20% data labeling. We first want to highlight that, in *all* the experiments, MAL achieves a higher mean accuracy in the beginning *before* selecting instances for labeling due to the effective semi-supervised learning strategy performed during adversarial training of F and C . We improve the state-of-the-art by more than 100% increase in the gap between the accuracy achieved by the previous state-of-the-art method (VAAL) and Random sampling. As can be seen in Fig. 3, this improvement can be also viewed in the number of samples required to achieve a specific accuracy. For instance, the accuracy of $41.92 \pm 0.75\%$ is achieved by MAL using 128K images whereas VAAL should be provided with almost 32K more images and Coreset and Random sampling with 64K more labeled images to obtain the same performance. Random sampling remains a competitive baseline as BALD performs below that.

MAL performance on iNaturalist2018. Figure 3 shows the accuracy achieved on iNaturalist2018 as a large-scale heavily long-tailed distribution with 8142 classes. Comparing the mean accuracy values across all the splits, shows that MAL evidently outperforms VAAL, Random sampling, Entropy, Coreset, and BALD by a large margin of nearly 4%. From the labeling-reduction point of view, this means that MAL requires 10% fewer annotations than all the baselines to obtain a fixed accuracy which is equivalent to 43K samples. This experiment highlights the value of evaluating on realistic datasets representing real-world difficulties associated with active learning. It surprisingly shows that all the previous baselines perform nearly identically when the class distribution is heavily imbalanced even though their performance appeared to be distinguishable on the ImageNet experiment. These results suggest active learning algorithms should be designed and tested on datasets representative of the real world.

MAL performance on CIFAR100. Figure 3 shows the performance of MAL on CIFAR100 which is a common benchmark used in active learning literature. MAL achieves mean accuracy of $44.8 \pm 0.4\%$ by using only 10% of the labels whereas the most competitive baseline, VAAL, obtains 41.6 ± 0.4 . All other baselines including Random, Coreset, Entropy, and BALD reach 40%. MAL consistently requires 2% less data which is equivalent to 1000 fewer number of labels compared to Random/Coreset/Entropy/BALD methods in order to achieve the same accuracy. This number is 1% for the most competitive baseline, VAAL, which performs slightly worse than MAL on the third and fourth splits when using 3000 and 4000 labeled images.

MAL performance on CIFAR100-Imbalanced. Prior work has largely considered using datasets with equally distributed images among classes [56, 51, 38, 66]. Our results on iNaturalist2018 dataset show that the majority of the algorithms in the literature fail in such scenarios, and hence, only evaluating on balanced datasets cannot accurately capture the performance of active learning algorithms. In an effort to mitigate this problem, we created an imbalanced version of CIFAR100 by keeping random *ratios* from each class, such that the least populated class has at least five instances while allowing for imbalances up to 100x. We use imbalance ratios of $\{10^{-2}, 10^{-1.5}, 10^{-1}, 10^{-0.5}, 10^0\}$. We use each ratio for 20 randomly chosen classes without replacement.

Figure 3 shows the results for the CIFAR100-Imbalanced experiment averaged over 10 runs, where the large error bars are the result of each run starting with a different imbalanced distribution. MAL outperforms the baselines across all the splits by an average margin of $1.94 \pm 0.41\%$ whereas Random sampling and Coreset perform similarly while BALD and Entropy perform worse. Due to the significant difference in the imbalance ratio across runs, the

performance of some methods including MAL, BALD, and Entropy appear to remain unchanged after adding the next split, but this is an artifact of averaging the substantially different performances from the different imbalance ratios. For each fixed imbalance ratio, the performance always improved by adding additional data. By looking at the number of labels required to reach a fixed performance, MAL achieves $9.74 \pm 0.40\%$ at the end of the first split using 2000 labeled samples whereas the best baseline (VAAL) only achieves $8.5 \pm 0.93\%$ at the end of the fourth split using 4000 labels.

4.2. MAL on image segmentation benchmarks

Implementation details. Similar to the image classification setup, we used random horizontal flips for data augmentation. Images and segmentation labels are resized to 224×224 , with nearest-neighbor interpolation being used on the segmentation map. For the initial labeled pool, we used 5% of the entire dataset, and for active learning, we use used a budget size of 5% of the full training set, which is equivalent to 350, 700, 1050, and 1400 samples. The architecture used in F is DRN [71], and C is a convolutional layer followed by an upsampling layer. Our setup for C is similar to what is used in the full segmentation model in the DRN paper. For our discriminator, instead of using a 3-layer MLP, we use a 3-layer CNN followed by a small fully-connected layer. Finally, for our choice of optimizer, we use Adam [30].

MAL performance on BDD100K. Figure 4 demonstrates our results on BDD100K dataset compared with two other baselines as well as the reference Random sampling. MAL consistently demonstrate better performance by achieving the highest mean IoU across different labeled data ratios. MAL is able to achieve %mIoU of $37.76 \pm 0.41\%$ using only 20% labeled data (1400 segmented images). In terms of required labels by each method, MAL needs 350 annotations to reach $33.41 \pm 0.29\%$ of mIoU whereas VAAL demands nearly 520, and Random sampling and Entropy require 700 labeled images to obtain the same mIoU. Considering the difficulties in full-frame instance segmentation, MAL is able to effectively reduce the required time and effort for such dense annotations.

5. Ablation study

Figure 5 shows our ablation study results. In this section, we take a deeper look into our model by performing an ablation study on CIFAR100 to inspect the contribution of the key modules in MAL as well as its sampling strategy. We compare our results with the most complete version of MAL and Random sampling. As shown by our ablations, each aspect of MAL is essential to its overall performance, indicating that the individual components operate in a complementary fashion to benefit the overall method.

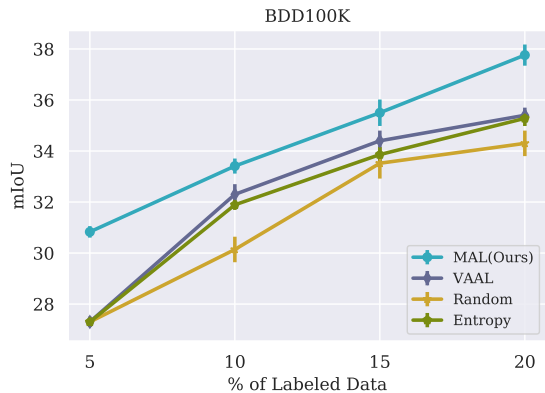


Figure 4: MAL performance on semantic segmentation task using BDD100K compared to VAAL [56], Entropy [66], and Random sampling. Best visible in color.

Ablating the minimax entropy optimization. For the first ablation, we eliminate the role of minimax entropy between F and C such that they only perform regular classification on the labeled data and no adversarial loss is computed using entropy. Note that we still train D on F 's feature space to predict the labeledness and use its prediction along with entropy values obtained by C to select samples for labeling. This setting performs worse than Random sampling and MAL by a large margin but it is the best performer among other ablations, showing the importance of using semi-supervised learning in active learning.

Ablating the discriminator. In this ablation, we eliminate D , and hence it is no longer trained on F 's latent space and is not used during the sample selection (i.e., we use samples with the highest entropy values obtained by C). This setting is the second best performing reduced version of MAL, which shows that the effect of using entropy values optimized adversarially is more critical than the discriminator's predictions.

Using uncertainty-based sampling only. This ablation is similar to removing D in terms of sampling criterion. However, here we still have a discriminator trained with F but we do not use its prediction to select our samples. The performance is slightly worse than also removing D from the training process but they both fail at sampling any informed sample beyond the first split.

Using diversity-based sampling only. This ablation removes the role of using entropy values obtained by C for the sampling strategy. This setting yields the poorest results showing that using entropy values obtained by a cosine-based classifier trained to maximize the entropy plays a major role in our overall architecture.

It is worth mentioning that the high-level outcome of our ablation study is aligned with those found in [56]. They found using unlabeled data (unsupervised reconstruction of

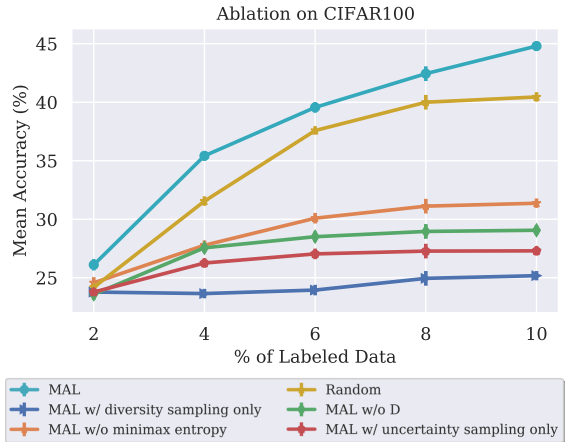


Figure 5: Ablation results on analyzing the effect of minimax entropy, discriminator (D), using entropy or discriminator's predictions for selecting samples in MAL. Results are averaged over 5 runs.

images in their case) had the largest effect on their overall performance. Similarly, we found the same for semi-supervised learning in MAL. However, we showed unlabeled data can be utilized more effectively when they are used in an adversarial game with labeled data.

5.1. Choice of the network architecture for F :

In order to assure MAL is insensitive to the ResNet18 architecture used in our classification experiments, we also used VGG [55] network architecture in MAL and the most competitive baseline (VAAL). Our results are shown in the appendix which clarifies that the choice of the architecture does not affect the performance gap between MAL and VAAL.

6. Conclusion

In this paper, we proposed a pool-based semi-supervised task-aware active learning algorithm, MAL, that learns a discriminative representation on the unlabeled data in an adversarial game between a feature extractor and a cosine similarity-based classifier while minimizing the expected loss on the labeled data. We train a binary classifier on this mixture of latent features so that it can distinguish between the labeled and unlabeled pool and implicitly learn the uncertainty for the samples deemed to be from the unlabeled pool. We introduced a hybrid sampling strategy that selects samples that are (i) most different from the already labeled data and (ii) farthest from class prototypes learned by a cosine-similarity classifier. We demonstrate state-of-the-art results on small and large-scale image classification (CIFAR100, ImageNet, iNaturalist2018) and a large scale semantic segmentation driving dataset (BDD100K).

References

- [1] David Arthur and Sergei Vassilvitskii. K-means++: The advantages of careful seeding. In *Proceedings of the Eighteenth Annual ACM-SIAM Symposium on Discrete Algorithms*, SODA '07, page 1027–1035, USA, 2007. Society for Industrial and Applied Mathematics. 3
- [2] Jordan T. Ash, Chicheng Zhang, Akshay Krishnamurthy, John Langford, and Alekh Agarwal. Deep batch active learning by diverse, uncertain gradient lower bounds. In *Eighth International Conference on Learning Representations (ICLR)*, April 2020. 3
- [3] Samaneh Azadi, Deepak Pathak, Sayna Ebrahimi, and Trevor Darrell. Compositional gan: Learning image-conditional binary composition. *arXiv preprint arXiv:1807.07560*, 2018. 3
- [4] William H Beluch, Tim Genewein, Andreas Nürnberger, and Jan M Köhler. The power of ensembles for active learning in image classification. In *Proceedings of the IEEE Conference on Computer Vision and Pattern Recognition*, pages 9368–9377, 2018. 1, 3
- [5] William H. Beluch, Tim Genewein, Andreas Nürnberger, and Jan M. Köhler. The power of ensembles for active learning in image classification. In *Proceedings of the IEEE Conference on Computer Vision and Pattern Recognition (CVPR)*, June 2018. 3
- [6] Klaus Brinker. Incorporating diversity in active learning with support vector machines. In *Proceedings of the 20th international conference on machine learning (ICML-03)*, pages 59–66, 2003. 3
- [7] Arantxa Casanova, Pedro O. Pinheiro, Negar Rostamzadeh, and Christopher J. Pal. Reinforced active learning for image segmentation. In *International Conference on Learning Representations*, 2020. 3
- [8] Wei-Yu Chen, Yen-Cheng Liu, Zsolt Kira, Yu-Chiang Frank Wang, and Jia-Bin Huang. A closer look at few-shot classification. In *International Conference on Learning Representations*, 2019. 2, 3, 4
- [9] Jia Deng, Wei Dong, Richard Socher, Lie-Jia Li, Kai Li, and Li Fei-Fei. ImageNet: A Large-Scale Hierarchical Image Database. In *CVPR09*, 2009. 5, 12
- [10] Josip Djolonga, Jessica Yung, Michael Tschannen, Rob Romijnders, Lucas Beyer, Alexander Kolesnikov, Joan Puigcerver, Matthias Minderer, Alexander D’Amour, Dan Moldovan, et al. On robustness and transferability of convolutional neural networks. *arXiv preprint arXiv:2007.08558*, 2020. 1
- [11] Alexey Dosovitskiy, Lucas Beyer, Alexander Kolesnikov, Dirk Weissenborn, Xiaohua Zhai, Thomas Unterthiner, Mostafa Dehghani, Matthias Minderer, Georg Heigold, Sylvain Gelly, et al. An image is worth 16x16 words: Transformers for image recognition at scale. *arXiv preprint arXiv:2010.11929*, 2020. 1
- [12] Sayna Ebrahimi, Mohamed Elhoseiny, Trevor Darrell, and Marcus Rohrbach. Uncertainty-guided continual learning with bayesian neural networks. In *International Conference on Learning Representations*, 2020. 3
- [13] Sayna Ebrahimi, Franziska Meier, Roberto Calandra, Trevor Darrell, and Marcus Rohrbach. Adversarial continual learning. *arXiv preprint arXiv:2003.09553*, 2020. 3
- [14] Xin Feng, Youni Jiang, Xuejiao Yang, Ming Du, and Xin Li. Computer vision algorithms and hardware implementations: A survey. *Integration*, 69:309–320, 2019. 1
- [15] Damien François. High-dimensional data analysis. In *From Optimal Metric to Feature Selection*, pages 54–55. VDM Verlag Saarbrücken, Germany, 2008. 3
- [16] Yoav Freund, H Sebastian Seung, Eli Shamir, and Naftali Tishby. Selective sampling using the query by committee algorithm. *Machine learning*, 28(2-3):133–168, 1997. 3
- [17] Yarin Gal and Zoubin Ghahramani. Dropout as a bayesian approximation: Representing model uncertainty in deep learning. In *international conference on machine learning*, pages 1050–1059, 2016. 3
- [18] Yarin Gal, Riashat Islam, and Zoubin Ghahramani. Deep bayesian active learning with image data. *arXiv preprint arXiv:1703.02910*, 2017. 1, 3, 5, 6
- [19] Yaroslav Ganin and Victor Lempitsky. Unsupervised domain adaptation by backpropagation. In *International conference on machine learning*, pages 1180–1189. PMLR, 2015. 4
- [20] Ran Gilad-Bachrach, Amir Navot, and Naftali Tishby. Query by committee made real. In *Advances in neural information processing systems*, pages 443–450, 2006. 3
- [21] Xavier Glorot and Yoshua Bengio. Understanding the difficulty of training deep feedforward neural networks. In *Proceedings of the thirteenth international conference on artificial intelligence and statistics*, pages 249–256, 2010. 6
- [22] Ian Goodfellow, Jean Pouget-Abadie, Mehdi Mirza, Bing Xu, David Warde-Farley, Sherjil Ozair, Aaron Courville, and Yoshua Bengio. Generative adversarial nets. In *Advances in neural information processing systems*, pages 2672–2680, 2014. 3, 4
- [23] Marc Gorriz, Axel Carlier, Emmanuel Faure, and Xavier Giro-i Nieto. Cost-effective active learning for melanoma segmentation. *arXiv preprint arXiv:1711.09168*, 2017. 1, 3
- [24] Yves Grandvalet and Yoshua Bengio. Entropy regularization., 2006. 3
- [25] Marian Grendár and Marián Grendár. Minimax entropy and maximum likelihood. *arXiv preprint math.PR/0009129*, 2000. 3
- [26] Gregory Griffin, Alex Holub, and Pietro Perona. Caltech-256 object category dataset. 2007. 12
- [27] Kaiming He, Xiangyu Zhang, Shaoqing Ren, and Jian Sun. Deep residual learning for image recognition. In *Proceedings of the IEEE conference on computer vision and pattern recognition*, pages 770–778, 2016. 5, 6
- [28] Edwin T Jaynes. Information theory and statistical mechanics. ii. *Physical review*, 108(2):171, 1957. 3
- [29] Ashish Kapoor, Kristen Grauman, Raquel Urtasun, and Trevor Darrell. Active learning with gaussian processes for object categorization. In *2007 IEEE 11th International Conference on Computer Vision*, pages 1–8. IEEE, 2007. 3
- [30] Diederik P Kingma and Jimmy Ba. Adam: A method for stochastic optimization. *arXiv preprint arXiv:1412.6980*, 2014. 7

- [31] Diederik P Kingma and Jimmy Ba. Adam: A method for stochastic optimization. In *International Conference on Learning Representations*, 2015. 6
- [32] Andreas Kirsch, Joost van Amersfoort, and Yarin Gal. Batchbald: Efficient and diverse batch acquisition for deep bayesian active learning. In H. Wallach, H. Larochelle, A. Beygelzimer, F. d'Alché-Buc, E. Fox, and R. Garnett, editors, *Advances in Neural Information Processing Systems 32*, pages 7026–7037. 2019. 1, 3
- [33] Alexander Kolesnikov, Lucas Beyer, Xiaohua Zhai, Joan Puigcerver, Jessica Yung, Sylvain Gelly, and Neil Houlsby. Big transfer (bit): General visual representation learning. *arXiv preprint arXiv:1912.11370*, 6, 2019. 1
- [34] Ksenia Konyushkova, Raphael Sznitman, and Pascal Fua. Introducing geometry in active learning for image segmentation. In *Proceedings of the IEEE International Conference on Computer Vision (ICCV)*, December 2015. 3
- [35] Andreas Krause, Pietro Perona, and Ryan Gomes. Discriminative clustering by regularized information maximization. *Advances in neural information processing systems*, 23:775–783, 2010. 3
- [36] Alex Krizhevsky and Geoffrey Hinton. Learning multiple layers of features from tiny images. Technical report, Citeseer, 2009. 5, 12
- [37] Solomon Kullback. *Information theory and statistics*. Courier Corporation, 1997. 3
- [38] Weicheng Kuo, Christian Häne, Esther Yuh, Pratik Mukherjee, and Jitendra Malik. Cost-sensitive active learning for intracranial hemorrhage detection. In *International Conference on Medical Image Computing and Computer-Assisted Intervention*, pages 715–723. Springer, 2018. 3, 7
- [39] Xin Li and Yuhong Guo. Adaptive active learning for image classification. In *Proceedings of the IEEE Conference on Computer Vision and Pattern Recognition*, pages 859–866, 2013. 3
- [40] David JC MacKay. Information-based objective functions for active data selection. *Neural computation*, 4(4):590–604, 1992. 3
- [41] Dwarikanath Mahapatra, Behzad Bozorgtabar, Jean-Philippe Thiran, and Mauricio Reyes. Efficient active learning for image classification and segmentation using a sample selection and conditional generative adversarial network. In *International Conference on Medical Image Computing and Computer-Assisted Intervention*, pages 580–588. Springer, 2018. 3
- [42] Alireza Makhzani, Jonathon Shlens, Navdeep Jaitly, Ian Goodfellow, and Brendan Frey. Adversarial autoencoders. *arXiv preprint arXiv:1511.05644*, 2015. 3
- [43] Christoph Mayer and Radu Timofte. Adversarial sampling for active learning. *arXiv preprint arXiv:1808.06671*, 2018. 3
- [44] Andrew Kachites McCallumzy and Kamal Nigamy. Employing em and pool-based active learning for text classification. In *Proc. International Conference on Machine Learning (ICML)*, pages 359–367. Citeseer, 1998. 3
- [45] Thomas Mensink, Jakob Verbeek, Florent Perronnin, and Gabriela Csurka. Metric learning for large scale image classification: Generalizing to new classes at near-zero cost. In *European Conference on Computer Vision*, pages 488–501. Springer, 2012. 3
- [46] Vinod Nair and Geoffrey E Hinton. Rectified linear units improve restricted boltzmann machines. In *ICML*, 2010. 6
- [47] Hieu T Nguyen and Arnold Smeulders. Active learning using pre-clustering. In *Proceedings of the twenty-first international conference on Machine learning*, page 79. ACM, 2004. 3
- [48] Hang Qi, Matthew Brown, and David G Lowe. Low-shot learning with imprinted weights. In *Proceedings of the IEEE conference on computer vision and pattern recognition*, pages 5822–5830, 2018. 3
- [49] Nicholas Roy and Andrew McCallum. Toward optimal active learning through monte carlo estimation of error reduction. *ICML, Williamstown*, pages 441–448, 2001. 3
- [50] Kuniaki Saito, Donghyun Kim, Stan Sclaroff, Trevor Darrell, and Kate Saenko. Semi-supervised domain adaptation via minimax entropy. In *Proceedings of the IEEE International Conference on Computer Vision*, pages 8050–8058, 2019. 3, 4
- [51] Ozan Sener and Silvio Savarese. Active learning for convolutional neural networks: A core-set approach. In *International Conference on Learning Representations*, 2018. 3, 5, 6, 7
- [52] Burr Settles. Active learning. *Synthesis Lectures on Artificial Intelligence and Machine Learning*, 6(1):1–114, 2012. 3
- [53] Burr Settles. Active learning literature survey. 2010. *Computer Sciences Technical Report*, 1648, 2014. 3
- [54] Claude Elwood Shannon. A mathematical theory of communication. *Bell system technical journal*, 27(3):379–423, 1948. 4
- [55] Karen Simonyan and Andrew Zisserman. Very deep convolutional networks for large-scale image recognition. *arXiv preprint arXiv:1409.1556*, 2014. 8
- [56] Samarth Sinha, Sayna Ebrahimi, and Trevor Darrell. Variational adversarial active learning. In *Proceedings of the IEEE/CVF International Conference on Computer Vision (ICCV)*, October 2019. 1, 2, 3, 5, 6, 7, 8, 12
- [57] Jake Snell, Kevin Swersky, and Richard Zemel. Prototypical networks for few-shot learning. In *Advances in neural information processing systems*, pages 4077–4087, 2017. 2
- [58] Jost Tobias Springenberg. Unsupervised and semi-supervised learning with categorical generative adversarial networks. *arXiv preprint arXiv:1511.06390*, 2015. 3
- [59] Chaofan Tao, Fengmao Lv, Lixin Duan, and Min Wu. Minimax entropy network: Learning category-invariant features for domain adaptation. *arXiv preprint arXiv:1904.09601*, 2019. 3
- [60] Simon Tong and Daphne Koller. Support vector machine active learning with applications to text classification. *Journal of machine learning research*, 2(Nov):45–66, 2001. 3
- [61] Toan Tran, Thanh-Toan Do, Ian Reid, and Gustavo Carneiro. Bayesian generative active deep learning. volume 97 of *Proceedings of the 36th International Conference on Machine Learning (ICML)*, pages 6295–6304, Long Beach, California, USA, 09–15 Jun 2019. PMLR. 3

- [62] Eric Tzeng, Judy Hoffman, Trevor Darrell, and Kate Saenko. Simultaneous deep transfer across domains and tasks. In *Proceedings of the IEEE International Conference on Computer Vision*, pages 4068–4076, 2015. 3
- [63] Eric Tzeng, Judy Hoffman, Kate Saenko, and Trevor Darrell. Adversarial discriminative domain adaptation. In *Proceedings of the IEEE Conference on Computer Vision and Pattern Recognition*, pages 7167–7176, 2017. 3
- [64] Grant Van Horn, Oisin Mac Aodha, Yang Song, Yin Cui, Chen Sun, Alex Shepard, Hartwig Adam, Pietro Perona, and Serge Belongie. The inaturalist species classification and detection dataset. In *Proceedings of the IEEE Conference on Computer Vision and Pattern Recognition (CVPR)*, June 2018. 5
- [65] Oriol Vinyals, Charles Blundell, Timothy Lillicrap, Daan Wierstra, et al. Matching networks for one shot learning. In *Advances in neural information processing systems*, pages 3630–3638, 2016. 2
- [66] D. Wang and Y. Shang. A new active labeling method for deep learning. In *2014 International Joint Conference on Neural Networks (IJCNN)*, pages 112–119, 2014. 1, 3, 5, 6, 7, 8
- [67] Dequan Wang, Evan Shelhamer, Shaoteng Liu, Bruno Olshausen, and Trevor Darrell. Fully test-time adaptation by entropy minimization. *arXiv preprint arXiv:2006.10726*, 2020. 3
- [68] Keze Wang, Dongyu Zhang, Ya Li, Ruimao Zhang, and Liang Lin. Cost-effective active learning for deep image classification. *IEEE Transactions on Circuits and Systems for Video Technology*, 27(12):2591–2600, 2017. 1, 3
- [69] Zheng Wang and Jieping Ye. Querying discriminative and representative samples for batch mode active learning. *ACM Transactions on Knowledge Discovery from Data (TKDD)*, 9(3):17, 2015. 3
- [70] Lin Yang, Yizhe Zhang, Jianxu Chen, Siyuan Zhang, and Danny Z Chen. Suggestive annotation: A deep active learning framework for biomedical image segmentation. In *International Conference on Medical Image Computing and Computer-Assisted Intervention*, pages 399–407. Springer, 2017. 3
- [71] Fisher Yu, Vladlen Koltun, and Thomas A Funkhouser. Dilated residual networks. In *CVPR*, volume 2, page 3, 2017. 5, 7
- [72] Fisher Yu, Wenqi Xian, Yingying Chen, Fangchen Liu, Mike Liao, Vashisht Madhavan, and Trevor Darrell. Bdd100k: A diverse driving video database with scalable annotation tooling. *arXiv preprint arXiv:1805.04687*, 2018. 5, 12
- [73] Jia-Jie Zhu and José Bento. Generative adversarial active learning. *arXiv preprint arXiv:1702.07956*, 2017. 3

Supplementary Material

Minimax Active Learning

A. Datasets

Table 1 shows a summary of the datasets used in our experiments. CIFAR100, ImageNet, and iNaturalist2018 are datasets used for image classification, while BDD100K was used for semantic segmentation. The budget for each dataset is the number of images that can be sampled at the end of each *split*.

Table 1: Summary of the utilized datasets

Dataset	#Classes	Train	Test	Initially Labeled	Budget	Image Size
CIFAR100 [36]	100	50000	10000	5000	2500	32×32
iNaturalist2018 [26]	8142	437513	24426	43751	43751	224×224
ImageNet [9]	1000	1281167	50000	64058	64058	224×224
BDD100K [72]	19	7000	1000	350	350	224×224

B. Choice of Architecture

Table 2 shows the performance of our method is robust to the choice of the architecture by having consistently better performance over VAAL [56] on CIFAR100 using VGG16-BN and ResNet18. As described in the main paper, task learner and F share the same CNN. For the classifier head in the task learner using VGG backbone, we used only one fully connected layer after the convolutional layers with $(512 \times 7 \times 7) \times 100$ where $(512 \times 7 \times 7)$ is the output size of the CNN and 100 is total number of classes in CIFAR100. This results in having 14.72M, 12.90M and 13.11M parameters in F , C , and D , respectively while T has 17.23M parameters. In our ResNet18 model, F , C , D , and T have 11.18M, 156.93K, 525.83K, and 11.23M parameters, respectively.

Table 2: Performance of MAL using ResNet18 and VGG16 on CIFAR100 versus VAAL on the same network architecture.

	2%	4%	6%	8%	10%
VAAL-VGG16 [56]	25.67 ± 0.98	35.67 ± 0.42	44.23 ± 1.32	47.89 ± 0.83	49.23 ± 0.61
MAL-VGG16 (Ours)	28.72 ± 0.73	39.84 ± 1.20	46.66 ± 0.91	49.97 ± 0.56	51.02 ± 0.76
VAAL-ResNet18 [56]	24.18 ± 0.48	32.44 ± 0.40	38.47 ± 0.25	40.89 ± 0.27	41.64 ± 0.39
MAL-ResNet18	26.14 ± 0.58	35.42 ± 0.32	39.56 ± 0.23	42.44 ± 0.63	44.81 ± 0.40